

# Additive coloring of thin, single crystalline MgO(001) films

Anastasia Gonchar,<sup>a</sup> Thomas Risse,<sup>\*a</sup> Elio Giamello<sup>b</sup> and Hans-Joachim Freund<sup>a</sup>

Received 12th April 2010, Accepted 19th June 2010

DOI: 10.1039/c0cp00197j

Electron bombardment of single-crystalline MgO(001) films has been shown to result in the formation of surface color centers. In this report we present an alternative way to produce surface color centers on single-crystalline MgO(001) films using additive Mg coloring.

Electron paramagnetic resonance (EPR) spectroscopy was used to prove the formation of surface paramagnetic color centers upon deposition of small amounts of Mg on MgO(001) films at 50 K. With increasing coverage the number of Mg induced color centers rises up to a coverage of about 0.03 monolayers and thereafter decreases with increasing Mg coverage. At high coverage and low temperatures metallic Mg clusters nucleate on the surface of the MgO(001) film as shown by infrared (IR) spectroscopy using CO as a probe molecule.

## 1. Introduction

The properties of metal oxides are often strongly modified by the presence of defects. In particular, point defects determine optical, electronic and transport properties of the materials.<sup>1</sup> For example, the color of an oxide is related to the presence of impurity atoms or vacancies in the lattice; the electronic properties of semiconductors are connected to the doping by impurity atoms. With respect to the surface of the materials defects play an important role for the chemical properties, which are a crucial ingredient in heterogeneous catalysis. A prominent case in which the chemistry of a point defect is believed to be decisive for the reaction, is the oxidative coupling of methane by Li-doped MgO.<sup>2</sup> A detailed understanding of the nature of point defects in oxides is therefore fundamentally important for the engineering of materials with well-defined properties.

Magnesium oxide is an ideal system in this respect, since it can be considered to be the prototype of an ionic oxide with simple rock-salt structure and it can be prepared as well ordered (001) terminated thin films. Despite the simplicity of MgO, the number of possible defect types in this crystal is considerable. Apart from morphological surface defects such as edges, kinks, steps, or dislocation lines, point defects such as cation or anion vacancies also need to be considered. The former are called V centers while the latter are known as F centers (from Farbe, the German word for color, thus the name color centers). Different numbers of electrons can be associated with such vacancies and the number is given with respect to the ideal lattice; e.g. a neutral anion vacancy contains two electrons and is called an F<sup>0</sup> center.

The study of bulk point defects in MgO and other alkaline earth oxides has been quite comprehensive in the past, see e.g. ref. 3–6. Substantial effort has been made to reveal the nature

and properties of the surface F<sub>s</sub> centers (the “s” subscript indicates a surface center).<sup>4,6–15</sup> In particular, paramagnetic F<sub>s</sub><sup>+</sup> centers containing a single electron were studied in great detail e.g. by electron paramagnetic resonance (EPR) spectroscopy. The F<sub>s</sub> centers were generated by different techniques, namely UV irradiation in the presence of adsorbed H<sub>2</sub>,<sup>10–14</sup> exposure of the oxide to H atoms,<sup>15</sup> irradiation,<sup>4,6</sup> and additive coloring with metal vapors having low ionization energy.<sup>7–9</sup> Depending on the preparation method neutral F<sub>s</sub><sup>0</sup> and/or paramagnetic F<sub>s</sub><sup>+</sup> are formed. In the case of the hydrogen treatments, so-called F<sub>s</sub><sup>+</sup>(H) centers are created, which were assigned to an electron trapped at a morphological defect (e.g. a reversed corner) stabilized by a proton close by. There is an ambiguity in the nomenclature of these centers with respect to the definition mentioned above, because it refers to a trapped electron rather than an anion vacancy as is classically meant by the term F center. However, we will adopt this nomenclature to simplify referral to the literature.

Due to their electronic properties surface F centers often-times react readily with adsorbed molecules.<sup>16–19</sup> Along the same lines it is also expected that metal particles nucleated at such F centers could have altered properties which in turn may result in different catalytic properties. The former effect was recently demonstrated showing that the nucleation of Au clusters at surface color centers leads to a charge transfer from the color center onto the Au cluster, thus, being negatively charged.<sup>20</sup> With respect to a change of the catalytic properties, experiments on size selected Au clusters indicated that their reactivity can also be altered by the presence of F centers.<sup>21</sup>

Due to the high reactivity of some of the surface F centers, investigations on powdered material suffer from the unavoidable interaction with background gases. A strategy to avoid the undesirable reactivity and gain more insight into geometric and electronic properties of surface color centers is the use of well defined single crystal surfaces under ultrahigh vacuum (UHV) conditions. Experimental studies to characterize such point defects at the atomic level are rather scarce. Recently, EPR and scanning tunneling microscopy (STM) studies have shown that F<sub>s</sub><sup>+</sup> centers as well as F<sub>s</sub><sup>0</sup> centers, generated by electron bombardment of single-crystalline MgO(001)

<sup>a</sup> Fritz-Haber-Institut der MPG, Department of Chemical Physics, Faradayweg 4-6, 14195 Berlin, Germany.  
E-mail: risse@fhi-berlin.mpg.de; Fax: +49 30 8413 4316;  
Tel: +49 30 8413 4218

<sup>b</sup> Dipartimento di Chimica Inorganica, Chimica Fisica e Chimica dei Materiali, Università di Torino, Via P. Giuria 9, 10125 Torino, Italy

thin films, are located on edges and corners of the MgO(001) islands.<sup>22</sup>

A few surface science studies on additive coloring by Mg on single-crystalline MgO films have been performed.<sup>23,24</sup> Kantorovich *et al.* employed metastable impact electron spectroscopy (MIES) on MgO(001) films after Mg deposition at 100 K and compared the experimental results with theoretical calculations. Even for the smallest amount of Mg, which is not defined in the paper,<sup>24</sup> a new feature at 2 eV above the valence band appeared in the band gap. Based on the theoretical calculations the peak around 2 eV found at low coverage was rationalized by the presence of Mg atoms or small clusters, while at high coverage work function measurements proved the existence of metallic Mg clusters. Indications for the presence of color centers were not found. Tegenkamp *et al.*<sup>23</sup> studied defects on MgO films, produced by evaporating monolayers of Mg at 300 K using electron energy loss spectroscopy (EELS). Two new features in the band gap of MgO were detected by EELS after Mg treatment and subsequent thermal treatment. These features were then tentatively assigned to color centers. In this work, we aim to provide direct experimental evidence for the formation of color centers upon additive coloring and report on a low temperature study (50 K) of Mg deposited on a single-crystalline MgO(001) thin film under UHV conditions. The interaction of additional Mg metal with a MgO(001) surface is characterized in the coverage range up to about 2 monolayers (ML). We focus on two main aspects. First, the deposition of small amounts of Mg will be discussed, which results in the formation of paramagnetic color centers as inferred from EPR spectroscopy. To this end the similarities and differences of  $F_s^+$  centers generated by the electron bombardment<sup>22</sup> and Mg additive coloring will be discussed. Secondly, infrared spectroscopy (IR) using CO as a probe molecule is used to characterize the fate of magnesium on MgO up to a coverage of 2 ML.

## 2. Experimental section

The experiments were performed using a UHV chamber equipped with standard UHV parts for sample preparation and characterization. Details of the experimental setup are described elsewhere.<sup>25</sup> The base pressure during experiments was below  $2 \times 10^{-10}$  mbar. Thin MgO films were grown on Mo(001) surfaces using established procedures.<sup>26</sup> In brief, the Mo substrate was cleaned by oxidation ( $1 \times 10^{-6}$  mbar of  $O_2$ ) at 1500 K and subsequent flashes to 2300 K. MgO(001) thin films of 20 monolayer (ML) thickness were prepared by evaporation of Mg in an oxygen background of  $1 \times 10^{-6}$  mbar and a substrate temperature of 600 K. The deposition rate was  $1 \text{ ML min}^{-1}$ . The sample was mounted on a He-cryostat, which allowed cooling down to 50 K. The temperature was measured by a thermocouple (type C) spot-welded to the upper edge of the Mo crystal using a commercial temperature controller (Schlichting Physikalische Instrumente). IR experiments were performed in grazing incidence reflection absorption geometry using a BioRad FTS 40 VM spectrometer. For the IRAS experiments CO was adsorbed at 50 K up to saturation coverage using a pin hole doser. High purity CO adsorbed on the surface was further purified using a liquid

nitrogen trap. The spectral resolution of the IR experiments was set to  $4 \text{ cm}^{-1}$  and 1000 scans were accumulated to obtain a reasonable signal-to-noise ratio. The cw-EPR spectra were measured at 50 K using a Bruker EMX X-Band spectrometer operating at approximately 9.65 GHz. For the current spectra a microwave power of 2 mW and a modulation amplitude of 4 G were used. Typically 100 scans were accumulated to obtain a reasonable signal-to-noise ratio. Mg atoms were deposited onto pristine MgO films at 50 K using the same commercial electron beam evaporator (Omicron EFM3) as for MgO film preparation. The deposited amount was calibrated by a quartz microbalance. The sample was biased to the voltage of the evaporant during Mg deposition to avoid acceleration of metal ions onto the surface.

## 3. Results and discussion

Fig. 1 presents EPR spectra collected after deposition of different amounts of Mg on a 20 ML thick MgO(001) film at 50 K. As a reference the bottom trace shows the background spectrum of the freshly prepared MgO film indicating no EPR signal within the detection limit of our EPR setup. This is in line with previous results and sets an upper bound for the number of paramagnetic color centers of approximately  $5 \times 10^{11} \text{ cm}^{-2}$ . After deposition of 0.005 ML Mg onto the pristine film, a signal appears around the  $g$ -value of the free electron ( $g_e = 2.0023$ ). The line width of the signal is 7 Gauss and remains constant within the temperature range 50–300 K while the intensity of the spectrum obeys Curie's law. The paramagnetic centers observed by EPR are located on the surface of the MgO film as verified by a complete quenching of the EPR signal upon adsorption of molecular oxygen at 50 K. The resonance line is almost symmetric and angular dependent measurements reveal neither a change in the line shape nor in resonance position. In principle, two origins of this signal are conceivable. On the one hand it is possible that this EPR signal arises from paramagnetic surface color centers in analogy to results from MgO powders. Those centers were also denoted as  $F_s^+$  centers. On the other hand one might think of conduction band ESR of small Mg particles. The latter, however, does not fit the experimental observations as the susceptibility, at least at higher temperatures such as 300 K, is expected to be determined by the small Pauli susceptibility of Mg and no Curie dependence of the intensity is expected.<sup>27,28</sup> In addition, the intensity of the signal expected based on the Pauli susceptibility of Mg is considerably smaller than the detection limit of the machine.<sup>29</sup> Surface color centers created by electron bombardment were characterized recently using EPR spectroscopy as well as STM and AFM.<sup>22,30,31</sup> At low temperatures these centers show a very similar EPR spectrum in terms of resonance position and line width as compared to Mg induced ones. It is thus tempting to identify the centers observed here with the ones obtained after electron bombardment. There are, however, differences in the spectroscopic behavior between the two situations. The first striking difference between these two preparations is the different temperature behavior of the EPR line width. While the Mg induced signal exhibits a 7 G wide signal between 50 and 300 K the electron bombarded system shows a

considerable narrowing (approx. 1.3 G) of the signal at high temperatures. This narrow width at higher temperatures compares well with the line width observed for well defined F centers on powders (e.g.  $F_s^+$  (H) center).<sup>32,33</sup> Thus, the larger line width observed here is attributed to inhomogeneous broadening caused by the presence of color centers at a variety of different local environments. Given the small  $g$ -tensor anisotropy, which was found to correspond to about 0.5 G for the electron induced color centers, it is not to be expected that this anisotropy can be picked up by angular dependent measurements of the inhomogeneously broadened line. In the case of the electron bombarded system it was shown that the F centers are predominately located at the edges of the MgO islands.<sup>22,30</sup> There the electrons are located in oxygen vacancies which are created through an electron stimulated desorption process as investigated by the Pfnür group.<sup>34</sup> High resolution STM measurements show that the number of oxygen vacancies present on the pristine film is very low if present at all. Therefore, it is not reasonable to assume that the Mg induced color centers also represent electrons located in anion vacancies in the classical sense. Instead it is very likely that the EPR signal observed here is due to electrons which are scavenged at morphological defects of the surface such as kinks or reversed corners. Theoretical calculations have shown that a stabilization of electrons is possible at a variety of sites having slightly different local environments which is reflected in slightly different  $g$ -values.<sup>35,36</sup> It is clear that within that scheme a positively charged Mg cation has to be stabilized on the surface as well. The data presented here allow no comments on the fate of these cations on the surface. An understanding of these processes at the atomic level is only possible applying complementary methods.

In Fig. 2, the peak-to-peak amplitude of the  $F_s^+$  center related signal as deduced from Fig. 1 is shown as a function of the Mg coverage. The use of the peak-to-peak amplitude as a measure of the intensity is justified by the absence of variations in line shape within this series of experiments. Furthermore,

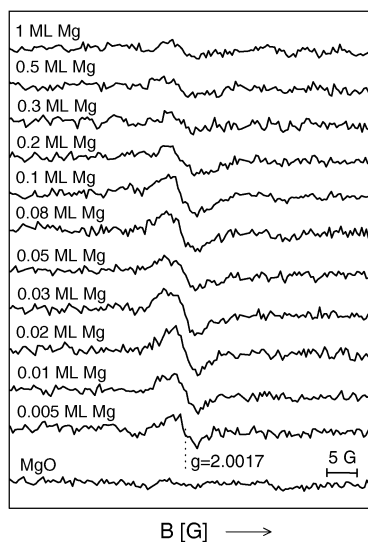


**Fig. 1** EPR spectra of 20 ML MgO(001) films. The bottom spectrum corresponds to the pristine film. The other traces were measured after additional Mg deposition of the given amounts.

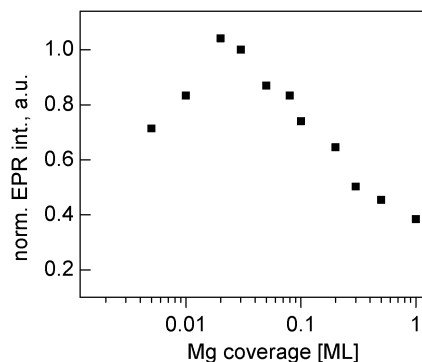


**Fig. 2** EPR peak-to-peak intensity of  $F_s^+$  centers as a function of the Mg coverage as derived from the spectra in Fig. 1.

the lack of changes in line shape excludes significant changes in the nature or environment of the underlying defects. The signal intensity increases from 0.005 ML to 0.03 ML Mg coverage by about 30% and decreases for higher exposures. This results in about the same signal intensity after additional deposition of 0.005 and 0.1 ML Mg. While a determination of the relative intensity of the spectra with respect to each other is rather accurate, an absolute calibration of this intensity is much more demanding. In order to give an estimate the signal obtained here was compared to spectra measured for Au atoms deposited at low temperatures.<sup>37</sup> In the case of Au it was shown that at low coverage a large fraction of the deposited material nucleates as atoms on the terraces of the MgO surface. Based on a correlation with EPR spectra of deposited Au atoms the maximal amount of Mg induced color centers can be estimated to be  $2\text{--}3 \times 10^{12} \text{ cm}^{-2}$ .

There are various possible explanations for the observed reduction of the EPR intensity for Mg coverage beyond 0.03 ML. Similar behavior was observed for electron induced  $F_s^+$  centers and the effect was explained by the formation of diamagnetic  $F_s^0$  centers, which are the more stable oxygen vacancies.<sup>30</sup> The formation of diamagnetic color centers cannot be excluded based on the EPR data and was also suggested early on.<sup>8</sup> To this end one has to bear in mind that the situation for the electron induced centers is different from Mg induced ones. While the doubly filled oxygen vacancies are more stable than the paramagnetic analogs, this is not true for electrons trapped at morphological defects. Thus, it cannot be considered as the natural explanation for the observed effect. Alternatively, the decrease of  $F_s^+$  center related signal intensity at higher coverage could be due to the formation of Mg clusters nucleating at or close to the trapping sites. This interpretation is corroborated by earlier temperature programmed desorption (TPD) measurements showing the growth of 3-dimensional Mg clusters from the very early stages of Mg deposition.<sup>38</sup>

In order to support the hypothesis of Mg cluster formation at high Mg coverage, the same system was investigated by IR spectroscopy using CO as a probe molecule. Carbon monoxide adsorption on MgO surfaces has been extensively studied experimentally and theoretically.<sup>39–44</sup> The infrared spectrum of thin MgO films saturated with CO at 30 K is characterized by a relatively sharp band at  $2152 \text{ cm}^{-1}$  exhibiting a shoulder

on the high frequency side and a pronounced feature at  $2138\text{ cm}^{-1}$ .<sup>42,43</sup> These bands are attributed to CO bound to regular MgO(001) terrace sites ( $2152\text{ cm}^{-1}$ ), morphological defects (shoulder around  $2170\text{ cm}^{-1}$ ), and an in-phase mode of the tilted molecules in high coverage phase on the MgO(001) terrace ( $2138\text{ cm}^{-1}$ ), respectively. At temperatures of about 50 K CO will reside on defect sites only. The corresponding IR spectrum at saturation coverage is characterized by a symmetric signal around  $2168\text{ cm}^{-1}$ , which corresponds to CO bound to the morphological defects of the MgO surface.

The IR spectra taken for different amounts of additionally deposited Mg are shown in Fig. 3. All spectra were measured after saturating the surface with CO at 50 K. The top curve shows the IR spectrum for CO on a pristine MgO film, which is characterized by a symmetric signal around  $2168\text{ cm}^{-1}$  in line with the previous study discussed above.<sup>42,43</sup> After the deposition of a small amount of Mg (0.1 ML) the spectral feature of the bare MgO film ( $2168\text{ cm}^{-1}$ ) changes only slightly. In particular no new feature associated with the added Mg metal can be found. The amplitude of the peak at  $2168\text{ cm}^{-1}$  is reduced and the line shape is altered. These changes in the spectrum can be explained by accommodating small amounts of Mg at line defects of MgO. After deposition of 1 ML of Mg a new rather broad band appears around  $2100\text{ cm}^{-1}$ . At the same time one can observe a substantial reduction in the intensity of the MgO related peak which is also shifted by  $4\text{ cm}^{-1}$  to the red (peak at  $2164\text{ cm}^{-1}$ ). The increase of Mg coverage to 2 ML results in a further reduction of the signal at  $2160\text{ cm}^{-1}$  while the band around  $2100\text{ cm}^{-1}$  becomes more pronounced. This new band at  $2100\text{ cm}^{-1}$  is in the typical range found for CO adsorbed on top to metal surfaces and it is thus assigned to CO bound to metallic Mg. The decrease in the intensity of CO bound to defects of the MgO film (band at  $2160\text{ cm}^{-1}$ ) can be explained by nucleation of Mg on these sites, hence blocking them for CO adsorption. The fact that the band at  $2160\text{ cm}^{-1}$  is still observed after deposition of 2 ML Mg points to the growth of 3-dimensional

(3D) Mg clusters, in line with the analysis of TPD data mentioned above.<sup>38</sup>

To the best of our knowledge, the stretching frequency of CO on magnesium clusters or single crystals has not yet been reported. Based on a simple analogy with other sp band metals such as Al it is expected that the interaction of the CO with Mg is rather weak and that the red shift, which is, within a simple Blyholder model,<sup>45</sup> due to a back donation into the  $\pi^*$ -orbital of the CO, should be small, too, due to the lack of appropriate filled orbitals. For Al(001) this results in a CO stretching frequency of  $2135\text{ cm}^{-1}$ .<sup>46</sup> The red shift observed here is significantly larger and closer to values found for CO on top of transition metals. The adsorption strength of CO on the Mg clusters can be estimated by annealing experiments. The three traces at the top of Fig. 4 show that the CO adsorbed on the Mg clusters (1 ML Mg on MgO) is already desorbed at 70 K confirming the expectation of a rather weak interaction of CO with Mg metal. The corresponding CO binding energy is estimated to be around 0.14 eV anticipating a desorption maximum in the given temperature window and applying the Redhead approximation.<sup>47</sup> In addition, a subsequent readsorption of CO at 50 K restores the original situation indicating reversible behavior, and thus stable Mg clusters, in this temperature range. The band at  $2168\text{ cm}^{-1}$ , corresponding to CO molecules bound to the MgO surface, undergoes a small shift to higher wavenumbers and decrease in intensity after annealing to 70 K. This indicates partial desorption of CO from the MgO surface, in agreement with previous work.<sup>42,43</sup> In a subsequent step the system was annealed to 110 K, which resulted in complete CO desorption from the surface as expected from previous TPD and IR results.<sup>42,43</sup> After CO readsorption at 50 K only one band appears at  $2168\text{ cm}^{-1}$ . This band is broader than the original one associated with CO adsorbed on morphological defects of the MgO surface. The lack of an IR band around  $2100\text{ cm}^{-1}$  indicates an irreversible change of the metallic Mg clusters after annealing to 110 K. This can be rationalized by a reaction of the metallic Mg clusters with the MgO surface resulting in the formation of a

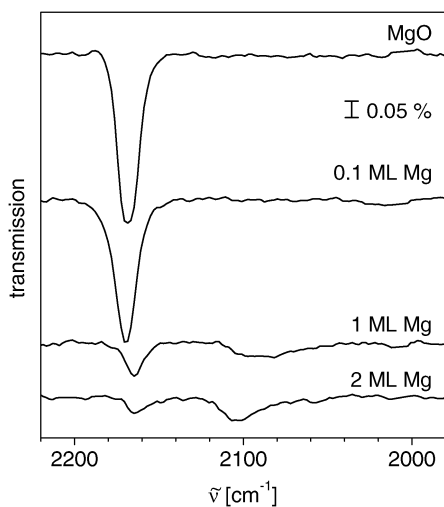


**Fig. 3** IR spectra taken for the bare MgO(001) film (top curve) and films additionally colored with different amounts of Mg coverage after CO saturation at 50 K. IR measurements were also performed at 50 K.

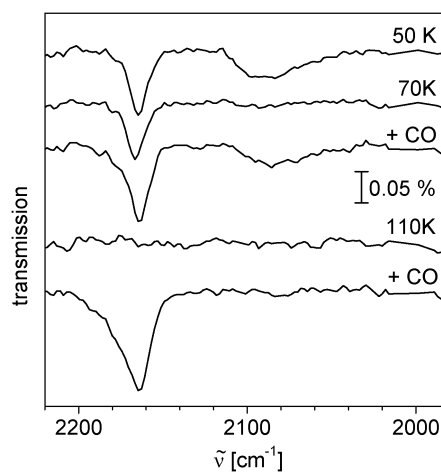


**Fig. 4** IR spectra of CO molecules adsorbed on a 1 ML Mg/20 ML MgO(100) film. The surface was first saturated with CO at 50 K. The sample was annealed to the indicated temperature. All spectra were measured at 50 K.

reduced MgO film. A detailed account of this effect goes beyond the scope of this paper and will be discussed elsewhere.

#### 4. Conclusions and outlook

The EPR experiments have shown the possibility of producing paramagnetic color centers,  $F_s^+$ , by deposition of small amounts of Mg at low temperatures on MgO(001) single-crystalline thin films. These centers are assigned to unpaired electrons trapped at morphological defects of the MgO surface in contrast to the color centers prepared by electron bombardment which were shown to be due to electrons trapped in oxygen vacancies. The number of Mg induced  $F_s^+$  centers goes through a maximum with increasing Mg coverage and decreases for Mg coverage above 0.03 ML. The maximum EPR intensity of these sites, which are stable beyond 300 K, corresponds to  $2\text{--}3 \times 10^{12} \text{ cm}^{-2}$ . The depletion of the color centers at higher coverage is attributed to the formation of metallic magnesium clusters in line with expectations based on previous investigations. The formation of metallic Mg clusters is confirmed by IR spectroscopy using CO as a probe molecule. This work demonstrates that paramagnetic excess electrons can be formed and characterized on well defined single crystal surfaces, which is an additional route to modifying surface properties and opens the way towards the investigation of other paramagnetic surface species such as suboxide ( $O^-$ ) anions.

#### Acknowledgements

A.G. thanks the IMPRS ‘‘Complex surfaces in Materials Science’’ for financial support. E.G. wants to thank the Alexander von Humboldt foundation for supporting his visit at the FHI. This work was partially supported by the European Union through the center of excellence IDECAT, and the COST program D41. The authors also acknowledge support from the Cluster of Excellence ‘‘Unifying Concepts in Catalysis’’ coordinated by the Technische Universität Berlin and funded by the Deutsche Forschungsgemeinschaft.

#### References

- 1 R. J. Tilley, *Principles and Applications of Chemical Defects*, Stanley Thornes, Cheltenham, 1998.
- 2 J. H. Lunsford, *Angew. Chem., Int. Ed. Engl.*, 1995, **34**, 970–980.
- 3 H. Weber, *Z. Phys.*, 1951, **130**, 392–402.
- 4 J. E. Wertz, J. W. Orton and P. Auzins, *Discuss. Faraday Soc.*, 1961, **31**, 140.
- 5 R. L. Nelson, A. J. Tench and B. J. Harmsworth, *Trans. Faraday Soc.*, 1967, **63**, 1427.
- 6 B. Henderson and J. E. Wertz, *Adv. Phys.*, 1968, **17**, 749–855.
- 7 A. Zecchina, D. Scarano, L. Marchese, S. Coluccia and E. Giamello, *Surf. Sci.*, 1988, **194**, 531–534.
- 8 E. Giamello, A. Ferrero, S. Coluccia and A. Zecchina, *J. Phys. Chem.*, 1991, **95**, 9385.
- 9 E. Giamello, D. Murphy, L. Ravera, S. Coluccia and A. Zecchina, *J. Chem. Soc., Faraday Trans.*, 1994, **90**, 3167–3174.
- 10 A. J. Tench and R. L. Nelson, *Trans. Faraday Soc.*, 1967, **63**, 2254.
- 11 R. L. Nelson and A. J. Tench, *Trans. Faraday Soc.*, 1967, **63**, 3039.
- 12 A. J. Tench and R. L. Nelson, *J. Colloid Interface Sci.*, 1968, **26**, 364.
- 13 R. L. Nelson, J. W. Hale, B. J. Harmsworth and A. J. Tench, *Trans. Faraday Soc.*, 1968, **64**, 2521.
- 14 A. J. Tench, *Surf. Sci.*, 1971, **25**, 625.
- 15 D. R. Smith and A. J. Tench, *Chem. Commun.*, 1968, 1113.
- 16 A. J. Tench, T. Lawson and J. Kibblewhite, *J. Chem. Soc., Faraday Trans. 1*, 1972, **68**, 1169.
- 17 M. Che and A. J. Tench, *Advances in Catalysis*, Academic Press, New York, 1983, vol. 32, pp. 1–148.
- 18 M. Chiesa, E. Giamello, M. C. Paganini, Z. Sojka and D. M. Murphy, *J. Chem. Phys.*, 2002, **116**, 4266–4274.
- 19 E. Giamello, D. Murphy, L. Marchese, G. Martra and A. Zecchina, *J. Chem. Soc., Faraday Trans.*, 1993, **89**, 3715–3722.
- 20 M. Sterrer, M. Yulikov, E. Fischbach, M. Heyde, H. P. Rust, G. Pacchioni, T. Risse and H.-J. Freund, *Angew. Chem., Int. Ed.*, 2006, **45**, 2630–2632.
- 21 B. Yoon, H. Häkkinen, U. Landman, A. S. Wörz, J. M. Antonietti, S. Abbet, K. Judai and U. Heiz, *Science*, 2005, **307**, 403–407.
- 22 M. Sterrer, E. Fischbach, T. Risse and H.-J. Freund, *Phys. Rev. Lett.*, 2005, **94**, 186101.
- 23 C. Tegenkamp, H. Pfnür, W. Ernst, U. Malaske, J. Wollschläger, D. Peterka, K. M. Schröder, V. Zielasek and M. Henzler, *J. Phys.: Condens. Matter*, 1999, **11**, 9943–9954.
- 24 L. Kantorovich, A. Shluger, J. Gunster, J. Stultz, S. Krischok, D. W. Goodman, P. Stracke and V. Kempter, *Nucl. Instrum. Methods Phys. Res., Sect. B*, 1999, **157**, 162–166.
- 25 J. Schmidt, T. Risse, H. Hamann and H.-J. Freund, *J. Chem. Phys.*, 2002, **116**, 10861–10868.
- 26 M. C. Wu, J. S. Corneille, C. A. Estrada, J. W. He and D. W. Goodman, *Chem. Phys. Lett.*, 1991, **182**, 472–478.
- 27 R. Denton, B. Mühlischlegel and D. J. Scalapino, *Phys. Rev. B: Solid State*, 1973, **7**, 3589.
- 28 R. Kubo, *J. Phys. Soc. Jpn.*, 1962, **17**, 975.
- 29 J. L. Millet and J. P. Borel, *Surf. Sci.*, 1981, **106**, 403–407.
- 30 M. Sterrer, M. Heyde, M. Novicki, N. Nilius, T. Risse, H. P. Rust, G. Pacchioni and H.-J. Freund, *J. Phys. Chem. B*, 2006, **110**, 46–49.
- 31 T. König, G. H. Simon, H. P. Rust, G. Pacchioni, M. Heyde and H.-J. Freund, *J. Am. Chem. Soc.*, 2009, **131**, 17544–17545.
- 32 M. Chiesa, M. C. Paganini, E. Giamello, D. M. Murphy, C. Di Valentin and G. Pacchioni, *Acc. Chem. Res.*, 2006, **39**, 861–867.
- 33 E. Giamello, M. C. Paganini, D. M. Murphy, A. M. Ferrari and G. Pacchioni, *J. Phys. Chem. B*, 1997, **101**, 971–982.
- 34 J. Kramer, W. Ernst, C. Tegenkamp and H. Pfnür, *Surf. Sci.*, 2002, **517**, 87–97.
- 35 D. Ricci, C. Di Valentin, G. Pacchioni, P. V. Sushko, A. L. Shluger and E. Giamello, *J. Am. Chem. Soc.*, 2003, **125**, 738–747.
- 36 M. Chiesa, M. C. Paganini, G. Spoto, E. Giamello, C. Di Valentin, A. Del Vitto and G. Pacchioni, *J. Phys. Chem. B*, 2005, **109**, 7314–7322.
- 37 M. Yulikov, M. Sterrer, T. Risse and H.-J. Freund, *Surf. Sci.*, 2009, **603**, 1622–1628.
- 38 J. Günster, J. Stultz, S. Krischok, D. W. Goodman, P. Stracke and V. Kempter, *J. Vac. Sci. Technol., A*, 1999, **17**, 1657–1662.
- 39 R. Wichtendahl, M. Rodriguez-Rodrigo, U. Härtel, H. Kühlenbeck and H.-J. Freund, *Phys. Status Solidi A*, 1999, **173**, 93–100.
- 40 G. Pacchioni, *Surf. Rev. Lett.*, 2000, **7**, 277–306.
- 41 Z. Dohnálek, G. A. Kimmel, S. A. Joyce, P. Ayotte, R. S. Smith and B. D. Kay, *J. Phys. Chem. B*, 2001, **105**, 3747–3751.
- 42 M. Sterrer, T. Risse and H.-J. Freund, *Surf. Sci.*, 2005, **596**, 222–228.
- 43 M. Sterrer, T. Risse and H.-J. Freund, *Appl. Catal., A*, 2006, **307**, 58–61.
- 44 J. W. He, J. S. Corneille, C. A. Estrada, M. C. Wu and D. W. Goodman, *J. Vac. Sci. Technol., A*, 1992, **10**, 2248–2252.
- 45 G. Blyholder, *J. Phys. Chem.*, 1964, **68**, 2772.
- 46 R. Ryberg, *Phys. Rev. B: Condens. Matter*, 1988, **37**, 2488.
- 47 P. A. Redhead, *Vacuum*, 1962, **12**, 203–211.